

# Ru-Hbpp-Based Water-Oxidation Catalysts Anchored on Conducting Solid Supports\*\*

Joaquim Mola, Elena Mas-Marza, Xavier Sala, Isabel Romero,\* Montserrat Rodríguez, Clara Viñas, Teodor Parella, and Antoni Llobet\*

The oxidation of water to molecular dioxygen is an important reaction both from a biological<sup>[1]</sup> and technological point of view, especially with regard to the development of commercial light-harvesting devices for the photo-production of H<sub>2</sub>.<sup>[2]</sup> Only a few complexes characterized at a molecular level have been described in the literature to be capable of catalytically oxidizing water to molecular dioxygen.<sup>[3]</sup> Dinuclear Ru-polypyridyl type complexes with different bridging ligands have been shown to give good performances in the homogeneous phase, although their performance in terms of TON (turnover number) is still far from a potential commercial application. It is thus very important to understand not only the reaction pathways through which those catalytic cycles proceed but also the deactivation process that leads to the decomposition of intermediates and stops the desired catalytic cycle.

The oxidation of water to molecular dioxygen is a highly demanding reaction for a catalyst since it is very complex from a mechanistic perspective and also because it is an uphill reaction with a very high thermodynamic potential. For this reason, deactivation pathways involving intermolecular catalyst–catalyst interactions are invoked in most reactions in the homogeneous phase whereby the polypyridyl ligands are oxidized<sup>[4]</sup> and the catalyst is destroyed. We have recently described the dinuclear cationic Ru catalyst [Ru<sub>2</sub><sup>II</sup>(μ-bpp)-

(trpy)<sub>2</sub>(H<sub>2</sub>O)<sub>2</sub>]<sup>3+</sup> (**3'**; bpp = bis(2-pyridyl)pyrazolato anion; trpy = 2,2':6',2''-terpyridine), which presents a relatively good performance with regard to its capacity to oxidize water to molecular dioxygen.<sup>[5]</sup> The main difference with the blue dimer reported by Meyer et al.<sup>[6]</sup> is the bridging ligand that determines the electronic coupling between the two Ru centers, the relative disposition of the active Ru=O groups, and the flexibility of the molecule.

We have undertaken a project to anchor our Ru catalyst onto solid supports in order to get a deeper insight into the potential deactivation pathways that lead to decomposition and also to demonstrate the viability of the reaction with the catalyst in the solid state. This would subsequently allow the catalyst to be incorporated into complex devices for solar energy harvesting based on water splitting.<sup>[7]</sup> The anodic electropolymerization of N-substituted pyrroles is a very convenient means of anchoring redox-active metal complexes onto conducting solid supports.<sup>[8]</sup> Thus, we have used the modified trpy ligand 4'-(para-pyrrolylmethylphenyl)-2,2':6',2''-terpyridine (t-trpy) to synthesize the cationic complex [Ru<sub>2</sub>(μ-bpp)(μ-OAc)(t-trpy)<sub>2</sub>]<sup>2+</sup> (**2**; Figure 1) in an

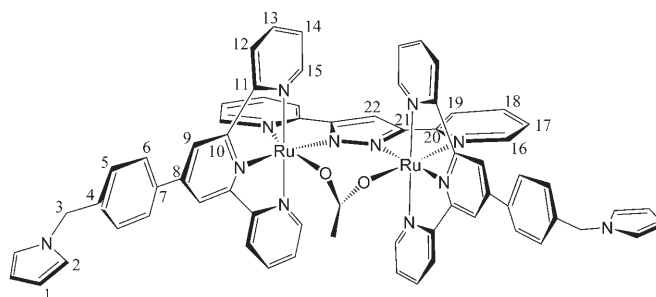


**Figure 1.** Structure of the cationic complex [Ru<sub>2</sub>(μ-bpp)(μ-OAc)(t-trpy)<sub>2</sub>]<sup>2+</sup> (**2**) with NMR labeling scheme.

analogous manner to the acetato precursor which, under acidic conditions, leads to **3'** (see the Supporting Information for a detailed description of the synthesis and spectroscopic and electrochemical characterization).

The acetato bridging ligand of **2** is substituted by two aqua ligands under acidic conditions to generate [Ru<sub>2</sub>(μ-bpp)(t-trpy)<sub>2</sub>(H<sub>2</sub>O)<sub>2</sub>]<sup>3+</sup> (**3**), whose metal centers have very similar chemical properties to those of **3'** since the new t-trpy ligand does not influence the intrinsic electronic and steric characteristics. However, the t-trpy pyrrole group polymerizes under sufficiently anodic potentials to generate a material that remains firmly attached to the surface of the electrode. We have selected two radically different surfaces to anchor our

[\*] J. Mola, Dr. I. Romero, Dr. M. Rodríguez  
Departament de Química, Universitat de Girona  
Campus de Montiliví, 17071 Girona (Spain)  
Fax: (+972) 0418.150  
E-mail: dir.depquimica@udg.edu  
Homepage: <http://www.udg.edu/depq>

Dr. E. Mas-Marza, Dr. X. Sala, Prof. A. Llobet  
Institute of Chemical Research of Catalonia (ICIQ)  
Av. Països Catalans 16, 43007 Tarragona (Spain) and Departament de Química, Universitat Autònoma de Barcelona  
Cerdanyola del Vallès, 08193 Barcelona (Spain)

Prof. C. Viñas  
Institut de Ciència de Materials de Barcelona (CSIC)  
Cerdanyola del Vallès, 08193 Barcelona (Spain)

Dr. T. Parella  
Servei de RMN Universitat Autònoma de Barcelona  
Cerdanyola del Vallès, 08193 Barcelona (Spain)

[\*\*] This research was financed by Solar-H<sub>2</sub> (EU 212508), the MEC (Spain) through projects Consolider Ingenio 2010 CSD2006-0003, CTQ2007-67918, and CTQ2007-60476. J.M. is grateful for the award of a doctoral grant from CIRIT Generalitat de Catalunya. Dr. E. Palomares from ICIQ is thanked for a gift of FTO electrodes. Hbpp = 3,5-bis(2-pyridyl)pyrazole.

Supporting information for this article is available on the WWW under <http://dx.doi.org/10.1002/anie.200704912>.

catalyst: vitreous carbon sponges (VCS) and fluorine-doped tin oxide (FTO). Figure 2 (top) shows the growth of FTO/poly-**2** over 30 repetitive scans from 0.0 to 1.2 V vs. SSCE. Once generated, the FTO/poly-**2** was soaked in a 0.1 M triflic

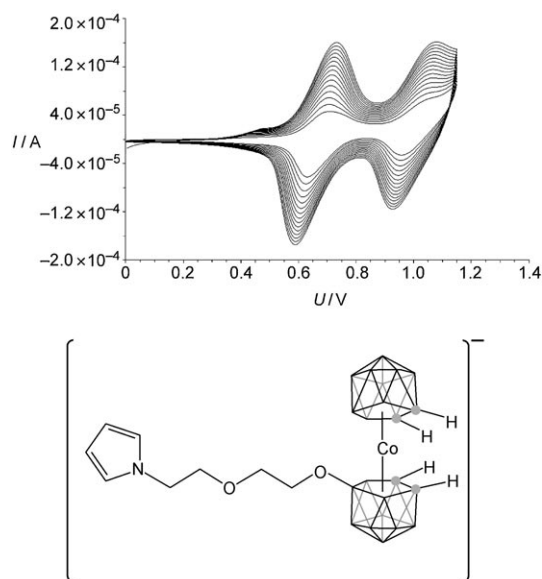


**Figure 2.** Top: growth of an FTO/poly-**2** film ( $\Gamma = 1.0 \times 10^{-9}$  mol cm $^{-2}$ ) over 30 repetitive scans between 0.0 and 1.2 V vs. SSCE, obtained using a 0.2 M solution of **2** in CH $_2$ Cl $_2$  ( $\mu = 0.1$  M tetrabutylammonium hexafluorophosphate (TBAH);  $\nu = 0.05$  V s $^{-1}$ ; FTO electrode area: 1.0  $\times$  1.0 cm $^2$ ). Bottom: structure of the anionic cobaltabisdicarbollide complex **4** containing a covalently bonded N-substituted pyrrole monomer.

acid solution to exchange the bridging acetato ligand for solvent molecules and generate the diaqua complex FTO/poly-**3**. The UV/Vis spectrum of FTO/poly-**3**, where the two Ru metals are both in oxidation state II, as well as the spectrum of their higher oxidation states (up to III, IV), which can be generated either chemically (with Ce $^{IV}$ ) or electrochemically, are remarkably similar to its homologue, the spectrum of **3'** in the homogeneous phase (see the Supporting Information). Similarly, the redox potentials of the different oxidation states of the anchored catalyst FTO/poly-**3** are also very similar to those obtained with its homologue **3'** but are slightly anodically shifted and have the II, II/II, III and II, III/III, III redox potentials fused into a single wave due most likely to the electrode geometry (see the Supporting Information). Thus, the UV/Vis spectra and electrochemical properties clearly show the existence of the same pattern for the different redox states in the thin films and in the homogeneous phase, which means that the process through which the higher oxidations are accessed is basically the same. A similar strategy was used to prepare VCS/poly-**3**.

To further separate the catalytically active species on the solid support we also prepared co-polymers with robust nonactive redox species that act as a diluting agent. We chose the N-substituted pyrrolic anionic cobaltabisdicarbollide complex **4** (Figure 2, bottom) for this purpose as it has been found recently to inhibit polypyrrole backbone oxidation,<sup>[9]</sup> which in our particular case would also be detrimental. The copolymers FTO/poly(**3-co-4**) were prepared by electropolymerization of solutions containing a 1:1 molar ratio of both monomers and were characterized spectroscopically and electrochemically. The ratio of monomers incorporated into the polypyrrolic backbone was evaluated by UV/Vis spectroscopy and turned out to be roughly 1:1, thereby indicating that the rate of polymerization of both monomers is practically the same. Table 1 shows the performance of the Hbpp-based water-oxidation catalysts in the homogeneous phase and the new polypyrrolic materials anchored onto the FTO and VCS solid supports.

The oxidation process is much faster in the homogeneous phase (Table 1, entries 1 and 2) than in the heterogeneous phase (Table 1, entries 3–5), as expected. Within the heterogeneous phase catalysis, the VCS catalyst is slower than the FTO one, thereby clearly indicating that diffusion processes within the solid matrix are the rate-determining step for the reaction. It is also important to note the overall improved performance of the catalyst in the heterogeneous phase with respect to the homogeneous phase. Another differentiating feature is that the anchored catalyst can be reutilized several times whereas in the homogeneous phase it cannot. Furthermore, CV clearly shows that the nature of the deactivated species is different. Thus, a wave is observed at 0.57 V in the

**Table 1:** Catalytic performance of the Ru catalyst in the homogeneous phase and anchored onto solid supports in 0.1 M solutions of triflic acid at room temperature.

Entry	Catalyst	Mols Ru cat. $\times 10^9$	Mols Ce $^{IV} \times 10^6$ <sup>[a]</sup>	TON <sup>[b]</sup>	$\nu_{O_2}$ <sup>[c]</sup>
1	<b>3'</b> <sup>[d]</sup>	1828	186 (102)	18.6	$2.5 \times 10^{-11}$
2	<b>3'</b> <sup>[e]</sup>	167	857 (5132)	22.9	$8.65 \times 10^{-10}$
3	VCS/poly- <b>3</b>	3.1	3.6 (1162)	41 <sup>[f]</sup> (32 + 9)	$6.25 \times 10^{-12}$
4	FTO/poly- <b>3</b>	1.0	3.6 (3600)	76	$1.2 \times 10^{-11}$
5	FTO/poly-( <b>3-co-4</b> )	0.5	1.8 (3600)	250 <sup>[g]</sup> (130 + 101 + 19)	$1.1 \times 10^{-11}$

[a] [Ce $^{IV}$ ]/[Cat] molar ratio in parentheses. [b] Turnover number. [c] Mols of O $_2$  generated per second. See the Supporting Information for techniques used to measure O $_2$ . [d] In the homogeneous phase with a total volume of 2 mL (see ref. [5]). [e] Experiment performed under the same conditions as for entry 1 but changing the amount of catalyst and oxidant as indicated. [f] Reutilized by adding the same amount of Ce $^{IV}$  after rinsing with 0.1 M triflic acid and removing liquids and gases under vacuum overnight. [g] After two reutilizations in the same manner as in [f].

homogeneous phase whereas in the heterogeneous phase a new wave is observed at 0.75 V (see the Supporting Information), thereby pointing to distinct deactivation reaction pathways.

Unfortunately we have still not been able to characterize the deactivated catalyst species structurally, although we have initiated a project in this direction. Another interestingly different aspect of the process in the homogeneous phase vs. the heterogeneous phase is the effect of increasing the [Ce $^{IV}$ ]/[Cat] ratio. In homogeneous phase this affects the TON slightly but increases the initial rates, whereas in the

heterogeneous phase the rates remain practically the same but the TON increases enormously, again manifesting the different nature of the two processes. Within the heterogeneous phase (Table 1, entries 3 and 4), the performance of the Ru catalyst increases dramatically as site dilution increases. This clearly points to the importance of catalyst–catalyst deactivation pathways that might involve oxidation of the  $\text{bpp}^-$  and/or  $\text{trpy}$  ligands, as has been proposed previously for other systems. This observation clearly shows the importance of the site isolation concept.<sup>[10]</sup> Entry 5 in Table 1 shows the spectacular performance of the new material containing the cobaltabisdicarbollide monomer, which prevents backbone oxidation and further dilutes the Ru catalyst. We have also shown that these new materials, as expected, are also capable of oxidizing water to molecular dioxygen electrocatalytically ( $E_{\text{app}} = 1.17 \text{ V}$  vs. SSCE), with a TON of 120 being obtained for VCS/poly-3 (see the Supporting Information for more details).

In conclusion, a homologue of the water-oxidation catalyst **3'** has been anchored onto two conducting solid supports whereupon its performance dramatically improves due to the minimization of catalyst–catalyst and catalyst–support interactions. Under the best conditions (Table 1, entry 5) the catalyst is capable of oxidizing water to molecular dioxygen with a TON of 250, which constitutes the best TON ever reported in the heterogeneous phase using a chemical oxidant. The present work also demonstrates the feasibility of building a solid-state device for the oxidation of water to molecular dioxygen that can be integrated, via a modular assembly, into a larger device for the photo-production of  $\text{H}_2$  and thus it also constitutes a step forward in this field.

### Experimental Section

$[\text{Ru}_2(\mu\text{-Cl})(\mu\text{-bpp})(\text{t-trpy})_2](\text{PF}_6)_2 \cdot 3\text{H}_2\text{O}$  (**1**)( $\text{PF}_6$ )<sub>2</sub>·3H<sub>2</sub>O): This compound was prepared in the same manner as described for **1'**, but using t-trpy instead of trpy.<sup>[9]</sup> Yield: 0.160 g (36%).

$[\text{Ru}_2(\mu\text{-OAc})(\mu\text{-bpp})(\text{t-trpy})_2](\text{PF}_6)_2 \cdot 4\text{H}_2\text{O}$  (**2**)( $\text{PF}_6$ )<sub>2</sub>·4H<sub>2</sub>O): Complex **1**·3H<sub>2</sub>O (0.083 g, 0.054 mmol) and sodium acetate (0.015 g, 0.108 mmol) were dissolved in 20 mL of acetone/water (3:1) and heated at reflux for 2 h. The resulting solution was filtered and a few drops of saturated aqueous  $\text{NH}_4\text{PF}_6$  added. The solid that precipitated upon reducing the volume was washed with cold water and diethyl ether. Yield: 0.067 g (80%).

Measurement of  $\text{O}_2$ : Oxygen evolution in the homogeneous phase was measured by analyzing the concentration of the gas phase with a GC equipped with a TCD detector. In this case the reactions were finished in less than 30 min. Oxygen evolution in the heterogeneous phase was measured in solution with a Hansatech Oxygraph System. The measurements were performed over a period of 12–14 h.

Analytic, spectroscopic, and electrochemical data are presented as Supporting Information.

Received: October 23, 2007

Revised: March 7, 2008

**Keywords:** heterogeneous catalysis · oxidation · ruthenium · water chemistry

- [1] a) J. Yano, J. Kern, K. Sauer, M. J. Latimer, Y. Pushkar, J. Biesiadka, B. Loll, W. Saenger, J. Messinger, A. Zouni, V. K. Yachandra, *Science* **2006**, *314*, 821; b) M. Haumann, P. Liebisch, C. Müller, M. Barra, M. Grabolle, H. Dau, *Science* **2005**, *310*, 1019.
- [2] R. Eisenberg, D. G. Nocera, *Inorg. Chem.* **2005**, *44*, 6799.
- [3] a) I. Romero, M. Rodriguez, C. Sens, J. Mola, M. H. Kollipara, L. Francas, E. Mas-Marza, L. Escriche, A. Llobet, *Inorg. Chem.* **2008**, *47*, 1824, and references therein; b) N. D. McDaniel, F. J. Coughlin, L. L. Tinker, S. Bernhard, *J. Am. Chem. Soc.* **2008**, *130*, 210; c) A. Sartorel, M. Carraro, G. Scorrano, R. De Zorzi, S. Geremia, N. D. McDaniel, S. Bernhard, M. Bonchio, *J. Am. Chem. Soc.* **2008**, *130*, 5006; d) Y. V. Geletii, B. Botar, P. Kögerler, D. A. Hillesheim, D. G. Musaev, C. L. Hill, *Angew. Chem.* **2008**, *120*, 3960; *Angew. Chem. Int. Ed.* **2008**, *47*, 3896.
- [4] a) K. Nagoshi, S. Yamashita, M. Yagi, M. Kaneko, *J. Mol. Catal. A* **1999**, *144*, 71; b) Y. K. Lai, K. Y. Wong, *J. Electroanal. Chem.* **1995**, *380*, 193.
- [5] C. Sens, I. Romero, M. Rodríguez, A. Llobet, T. Parella, J. Benet-Buchholz, *J. Am. Chem. Soc.* **2004**, *126*, 7798.
- [6] J. A. Gilbert, D. S. Eggleston, W. R. Murphy, Jr., D. A. Geselowitz, S. W. Gestern, D. J. Hodgson, T. J. Meyer, *J. Am. Chem. Soc.* **1985**, *107*, 3855.
- [7] a) F. Liu, T. Cardolaccia, B. J. Hornstein, J. R. Schoonover, T. J. Meyer, *J. Am. Chem. Soc.* **2007**, *129*, 2446; b) M. Grätzel, *Nature* **2001**, *414*, 338.
- [8] A. Deronzier, J. C. Moutet, *Acc. Chem. Res.* **1989**, *22*, 249.
- [9] a) C. Masalles, J. Llop, C. Viñas, F. Teixidor, *Adv. Mater.* **2002**, *14*, 826; b) J. Llop, C. Masalles, C. Viñas, F. Teixidor, R. Sillanpää, R. Kivekäs, *Dalton Trans.* **2003**, 556.
- [10] B. J. Hornstein, D. M. Dattelbaum, J. R. Schoonover, T. J. Meyer, *Inorg. Chem.* **2007**, *46*, 8139.